

## **D2.2 GRAVIMETRIC SURVEY**

# LOPÍN STRUCTURE, ONSHORE EBRO BASIN, SPAIN

Release Status: Final

Authors: Félix M. Rubio, Carmen Rey-Moral, Conxi Ayala, Arturo García García,  
Agustín González Durán, Jose María Llorente Delgado, Jose Francisco Mediato  
Arribas

Date: 27 July, 2022

Filename and Version: V2

Project ID Number: 101022664

PilotSTRATEGY (H2020- Topic LC-SC3-NZE-6-2020 - RIA)

## Document History

### Location

This document is stored in the following location:

|                 |   |
|-----------------|---|
| <b>Filename</b> | D2.2_PilotSTRATEGY_GravimetricSurvey  |
| <b>Location</b> | <a href="https://pilotstrategy.eu/about-the-project/work-packages/geo-characterisation">https://pilotstrategy.eu/about-the-project/work-packages/geo-characterisation</a> |

### Revision History

This document has been through the following revisions:

| Version No. | Revision Date                | Filename/Location stored: | Brief Summary of Changes |
|-------------|------------------------------|---------------------------|--------------------------|
| 1           | June 23 <sup>rd</sup> , 2022 |                           |                          |
| 2           | July 27 <sup>th</sup> , 2022 |                           |                          |
|             |                              |                           |                          |

### Authorisation

This document requires the following approvals:

| AUTHORISATION       | Name                             | Signature | Date     |
|---------------------|----------------------------------|-----------|----------|
| WP Leader           | Mark Wilkinson                   |           | 01/08/22 |
| Project Coordinator | Fernanda de Mesquita Lobo Veloso |           | 31/08/22 |

### Distribution

This document has been distributed to:

| Name | Title | Version Issued | Date of Issue |
|------|-------|----------------|---------------|
|      |       | PUBLIC         | 00/00/0000    |
|      |       |                |               |
|      |       |                |               |

© European Union, 2022

No third-party textual or artistic material is included in the publication without the copyright holder's prior consent to further dissemination by other third parties.

Reproduction is authorised provided the source is acknowledged.

Rubio et al. 2022. D2.2 Gravimetric Survey. Lopín structure, Onshore Ebro Basin, Spain. PilotSTRATEGY deliverable. EU H2020 PilotSTRATEGY project 101022664, report, pp 30.

### **Disclaimer**

The information and views set out in this report are those of the author(s) and do not necessarily reflect the official opinion of the European Union. Neither the European Union institutions and bodies nor any person acting on their behalf may be held responsible for the use which may be made of the information contained therein.



## Executive summary

Within the framework of the project “CO<sub>2</sub> Geological Pilots in Strategic Territories (pilotSTRATEGY)”, a gravimetric survey was carried out with the aim of improving the knowledge of the Lopín structure (Ebro Basin-onshore). The Lopín structure was previously characterized using existing vintage seismic lines and well-log data producing a 3D structural model, including the geometry and detailed distribution of the main geological units and faults, but some gaps and missing information were identified. The irregular distribution of the seismic lines did not allow verifying the structural closure of the reservoir in the southeast and north margins of the structure. Thus, the goal of the gravimetric survey (with a planned sampling of two gravimetric stations per km<sup>2</sup>) is to determine the extension of the structure and support the construction of a geological model based on 3D gravimetric modelling to verify its geometry.

To accomplish a gravimetric survey, it is necessary to create detailed topography maps with errors below certain standardized values. Moreover, the gravity data must be corrected to obtain the final Bouguer anomaly data, including corrections for altitude, terrain and the Bouguer correction.

The Bouguer anomaly map incorporates all the corrections and reveals lateral density variations in the Earth that are usually associated with geological structures. It displays the superposition of anomalies produced by many different sources at different depths. As our goal is located at a relatively shallow depth, we calculate the residual Bouguer anomaly map by subtracting the regional anomaly map from the Bouguer anomaly map.

The residual Bouguer anomaly map of the Lopín structure shows two relative elongated maxima with a NW-SE orientation in the centre, that extend to the southeast with less amplitude signal. The two gravimetric highs are bounded to the NE and SW by two gravimetric lows and to the NE and SE by shallow relative gravimetric lows with other larger gravimetric highs.

This gravimetric study, allowed filling the existing gaps of information and represents the first step to carry on the development, monitoring and implementation of this potential Pilot Site.

## Table of Contents

|   |           |
|---|-----------|
| <b>Document History</b> .....   | <b>1</b>  |
| <b>Location</b> .....   | <b>1</b>  |
| <b>Revision History</b> .....   | <b>1</b>  |
| <b>Authorisation</b> .....  | <b>1</b>  |
| <b>Distribution</b> .....   | <b>1</b>  |
| <b>Executive summary</b> .....  | <b>3</b>  |
| <b>1. Introduction</b> .....  | <b>5</b>  |
| <b>2. Gravimetric survey</b> .....  | <b>6</b>  |
| <b>2.1 Topographic survey using GNSS (Global Navigation Satellite System)</b> ..... | <b>7</b>  |
| 2.1.1 Control of repetitions.....   | 8         |
| <b>2.2 Gravimetric data acquisition</b> .....                                       | <b>11</b> |
| 2.2.1 Control of repetitions.....   | 12        |
| 2.2.2 Calculation of observed gravity .....   | 13        |
| <b>2.3 Calculation of gravimetric anomalies</b> .....                               | <b>14</b> |
| <b>2.4 Calculation of the Bouguer anomaly</b> .....                                 | <b>15</b> |
| 2.4.1 Normal gravity .....  | 15        |
| 2.4.2 Altitude correction (free air correction) .....                               | 16        |
| 2.4.3 Bouguer correction .....  | 16        |
| 2.4.4 Terrain correction .....  | 16        |
| 2.4.5 Bouguer anomaly.....  | 17        |
| <b>3. Analysis of gravimetric data</b> .....  | <b>18</b> |
| 3.1.1 Bouguer Anomaly map .....   | 18        |
| 3.1.2 Regional-Residual separation .....  | 19        |
| <b>4. Interpretation</b> .....  | <b>21</b> |
| <b>5. References</b> .....  | <b>25</b> |
| <b>6. Annex</b> .....   | <b>26</b> |

## 1. Introduction

The project “CO<sub>2</sub> Geological Pilots in Strategic Territories (pilotSTRATEGY)”, is a European Project in the framework of the 2020 Horizon call (CALL H2020-LC-SC3-2018-2019-2020).

The objective of the project is to present a proposal for the development, monitoring and implementation of three pilot sites for CO<sub>2</sub> storage in France, Portugal and Spain, and in lesser detail, in Poland and Greece. The proposal, one site for each country of the three main regions, will be based on the detailed geological characterization of the structure, static and dynamic modelling, the detection of associated risks, and social acceptance. The project is presented as a continuation of the STRATEGY CCUS (2019-2021) of the H2020 in which the IGME also participated.

In the case of Spain, two possible structures within saline aquifers were initially proposed and, after a year of detailed study, one of them will be selected to complete the project tasks and objectives. The proposed structures are:

- (1) **Onshore structure (LOPÍN):** Selected from previous work done by IGME, mainly on the ALGECO2 project. It is located in Aragón area, 50 km away of Zaragoza, in Belchite zone.
- (2) **Offshore structure:** Identified by Repsol based on existing 3D seismic and data from a former oil and gas permit.

The best alternative will be selected based on a multidisciplinary approach, i.e., taking into account technical, social, environmental and techno-economic points of view.

The Lopín structure was initially studied within the framework of the Project “Plan for the selection and characterization of favourable areas and structures for the geological storage of CO<sub>2</sub> in Spain” (ID 64055) within the Plan for the geological storage of CO<sub>2</sub> of the IGME “Plan ALgeCo2”. Moreover, it was studied supported by the Institute for the Restructuring of Coal Mining and the alternative development of the Mining districts (IRMC). The Lopín structure (Fig. 1) was characterized using available seismic lines and log data, achieving a 3D structural model of the Lopín subsurface structure, including the geometry and detailed distribution of the main geological units and faults (Mediato et al., 2015).

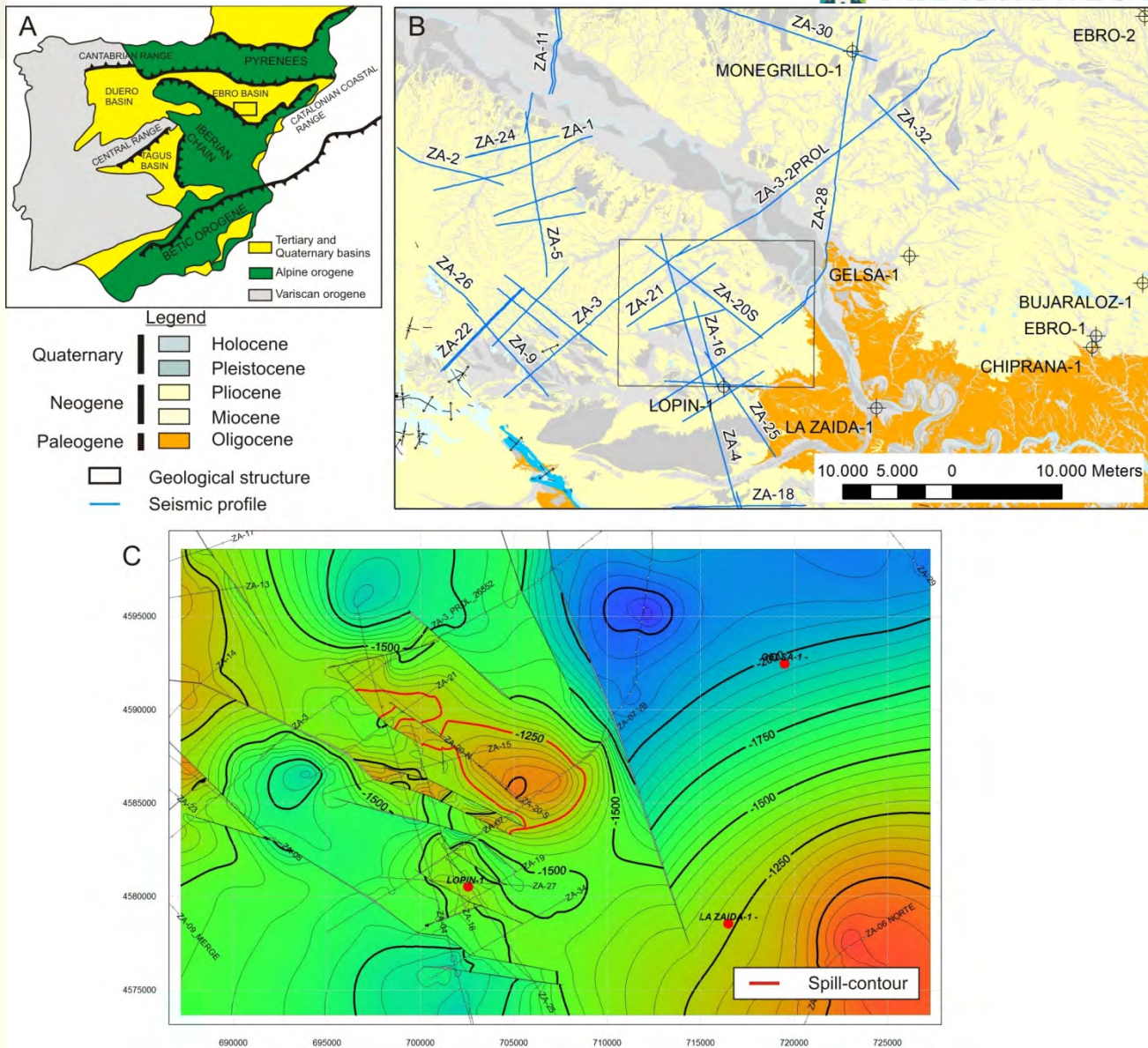


Figure 1: Location of the study area. B. Schematic geological map of the Lopin area with the legacy reflection seismic lines (in blue). C. Depth (meters above sea level) contour lines of Buntsandstein top with spill-contour marked in red (modified of Mediato et al., 2015).

However, some data-gaps and missing information were identified and, in the framework of this project, we will review and reprocess the existing information and obtain new field data. Among those, a new gravimetric survey was carried out, with a coverage of two gravimetric stations per km<sup>2</sup>. In addition, we performed eight more detailed gravimetric profiles (see Figure 2 for location).

## 2. Gravimetric survey

The new data were acquired between June and October 2021. Measurements were taken simultaneously at each station with the gravimeter and with Global Navigation Satellite System (GNSS) devices to obtain coordinates that optimize the data collection in the field.



Picture 1. Example of gravimetry and GPS measurement.

## 2.1 Topographic survey using GNSS (Global Navigation Satellite System)

In this work, the calculation of the coordinates are referred to the ETRS89 system and the calculation of normal gravity to the GRS80 geodetic system.

For the GPS data, a Triumph receiver from JAVAD GNSS was used in static mode. Gravimetry measurements were acquired simultaneously (see picture 1).

The GPS data had to be corrected with some fixed bases. We used Quinto and Zaragoza bases (from the ARAGEA network of the Government of Aragón, see Annex figures 1 and 2). Afterwards, the differential correction is carried out in the office during the post-processing. To calculate the coordinates of each point we used JUSTIN software developed by the Javad GNSS Company. The obtained coordinates are as follow:

- Latitude and longitude
- X and Y in UTM projection, Zone 30 North
- Ellipsoidal height

The calculation of the orthometric height is carried out through the Geodetic Applications Program (PAG v1.3) (<https://datos-geodesia.ign.es/PAG/instalador/>), developed by the National Geographic Institute (IGN). In this case, we used the geoid model EGM08REDNAP from the Instituto Geográfico Nacional (IGN, <https://www.ign.es/web/ign/portal>).

In accordance with the objectives of the work, the field data have a homogeneous distribution of 2 points/km<sup>2</sup>, except in the areas of the profiles where the number of points was increased (see Figure 2). In order to avoid edge effects, we added a 2 km-wide border, as a frame around the core study area, with a distribution of points of 1 point/2km<sup>2</sup>. The total number of points measured is 715 (see Figure 2).

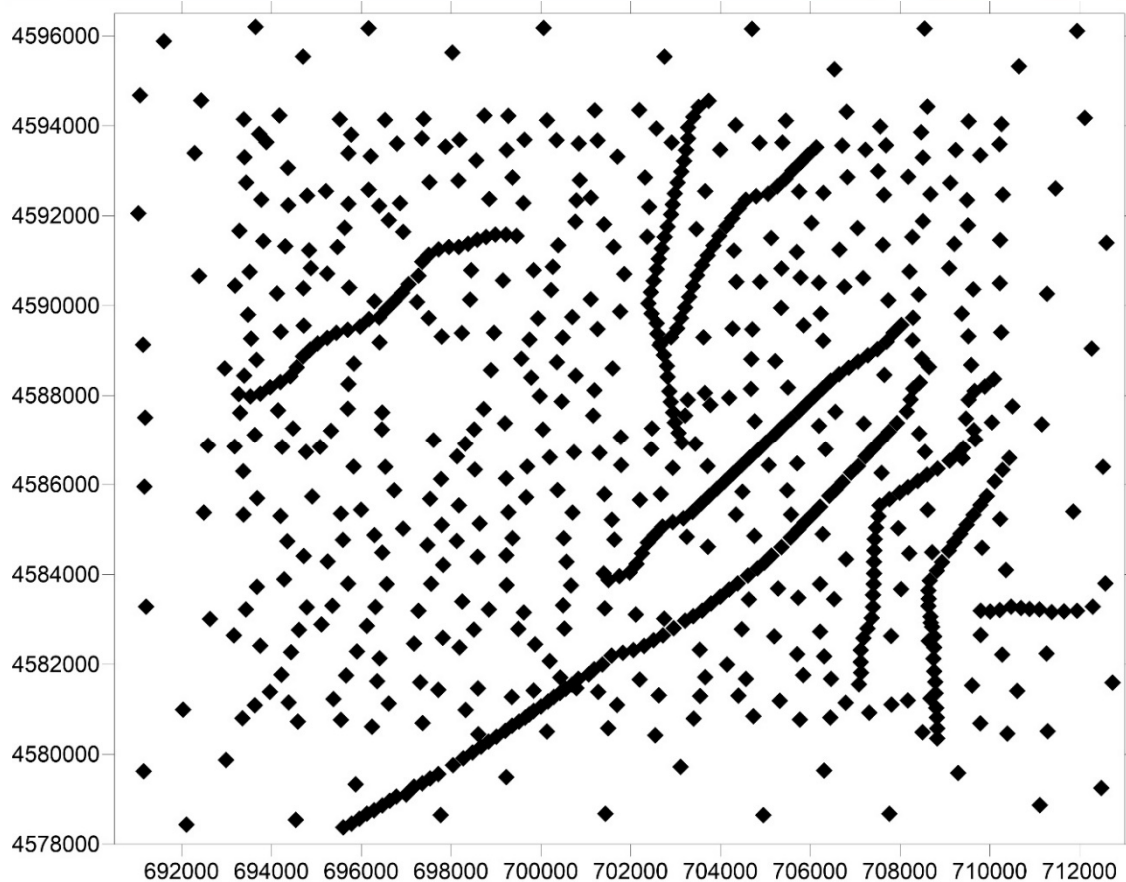


Figure 2. Location of the gravimetric stations. Coordinate system UTM ETRS89 H30N in meters.

### 2.1.1 Control of repetitions

To ensure the quality of the survey we used as reference the Spanish norm UNE 22-611-85: which is a standard for terrestrial geophysical prospecting, specifically to the gravimetric method. Following this norm: "the accuracy of the measurements will be controlled as follows: at least 5% of the stations will be measured twice in the course of different programs (we call program a working day)". In the case of gravimetric data, with this working scale of 1:10,000, the value of the root mean square error ( $E_{cm}$ ), for the repetitions of the X and Y coordinates in meters, must be less than +/- 10 m and for the Z dimension it must be less than +/- 0.2 m.

To calculate the root mean square error ( $E_{cm}$ ), we use the formula:

$$E_{cm} = \pm \sqrt{\frac{\sum d^2}{2N}}$$

where  $d$  is the difference between the first measurement and the repetition and  $N$  is the number of repeated points.

We achieved 74 (73 for coordinate z) repetitions, which represents 10.35% of the points of the survey, obtaining the following statistics:

X coordinate (UTM ETRS89 H30N) (Figure 3)

- 74 values (100%) below 0.50 m difference.
- Mean value of the differences 0.033 m.
- Mean square error of the repetitions 0.036 m.

Y coordinate (UTM ETRS89 H30N) (Figure 3)

- 74 values (100%) below 0.50 m difference.
- Mean value of the differences 0.038 m.
- Mean square error of the repetitions 0.036 m.

Z coordinate (orthometric) (Figure 3)

- 73 values (100%) below 0.50 m difference.
- Mean value of the differences 0.043 m.
- Mean square error of the repetitions 0.063 m.

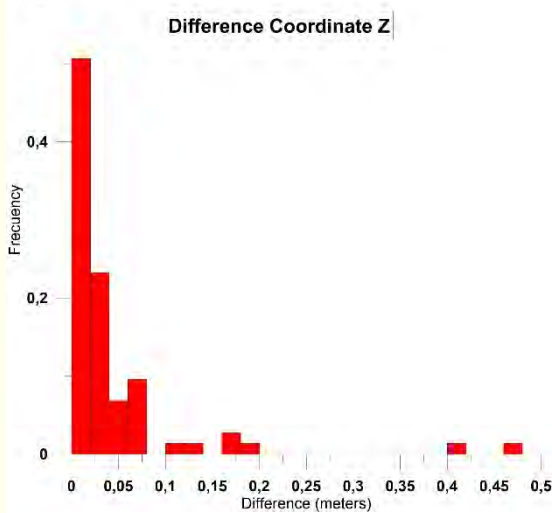
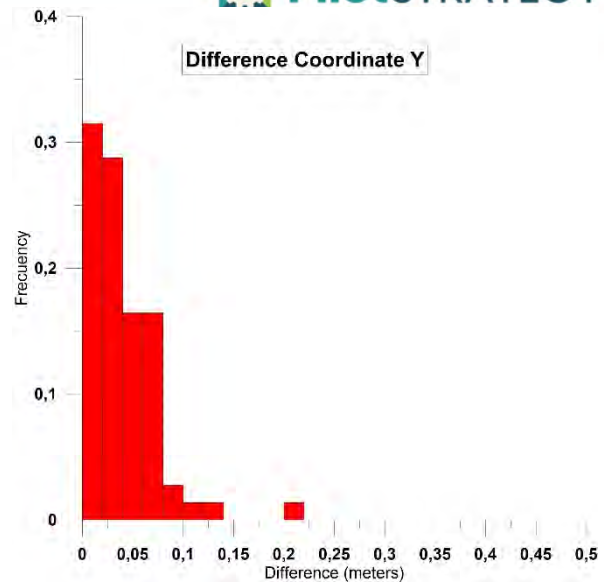
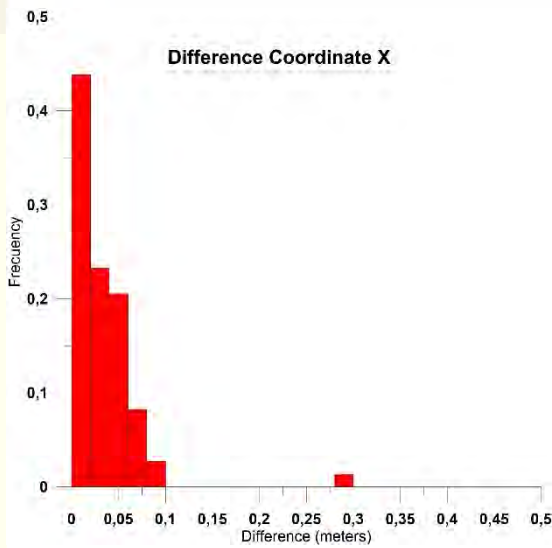


Figure 3. Differences for X, Y and Z coordinates. Axe X represents difference in meters, Axe Y represents relative frequency.

In fact, these repetitions refer to the behaviour of the instruments during the survey. In order to control the absolute value of the measurements, we measure some geodesic vertices (IGN database, <https://www.ign.es/web/ign/portal/gds-vertices/-/vertices-geodesicos/setTabNumber>) in the area, and incorporated the values to our survey. These points were used as control points of the accuracy achieved during the survey. We have used the geodesic vertices: nº 41281 Escudero, nº 41286 La Tosqueta and nº 41303 Carnero (see annex for details, Figs. 3 and 4).

The differences between the value of the geodesic vertices and the value measured in the survey are depicted in the table 1. The height is above sea level (orthometric) and referred to the ground (base of the vertices' body). The results are within the admissible error for this type of survey.

| Vertice            | IGN Coordinates |            |        | Survey Coordinates |            |        | Differences |       |      |
|--------------------|-----------------|------------|--------|--------------------|------------|--------|-------------|-------|------|
|                    | X               | Y          | Z      | X                  | Y          | Z      | X           | Y     | Z    |
| <b>Escudero</b>    | 704145,16       | 4581994,23 | 267,87 | 704145,13          | 4581994,50 | 267,79 | 0,03        | -0,27 | 0,08 |
| <b>La Tosqueta</b> | 704350,80       | 4590526,19 | 273,69 | 704350,94          | 4590526,00 | 273,67 | -0,14       | 0,19  | 0,02 |
| <b>Carnero</b>     | 707958,36       | 4585023,39 | 265,58 | 707958,44          | 4585024,00 | 265,54 | -0,08       | -0,61 | 0,04 |

Table 1. Differences between IGN geodesic vertices values, used as control points, and the points of the survey.

## 2.2 Gravimetric data acquisition

The acquisition of the gravimetric data was carried out using an Autograv Scintrex CG5 gravimeter.

To obtain the observed gravity, two locations with gravimetric value from the International Standardization Network 1971 (IGSN71) were used:

- 1) Station NGAB 635 from IGN (NAP 635 in Fig. 4), *Red Española de Nivelación de Alta Precisión* (REDNAP) network (see annex for more detail, Fig. 4).
- 2) A base was established inside the working area (see annex, Fig. 4), located in Quinto (Zaragoza). This base has been linked to the REDNAP station. The linkage between the new base and the REDNAP is shown in figure 4.

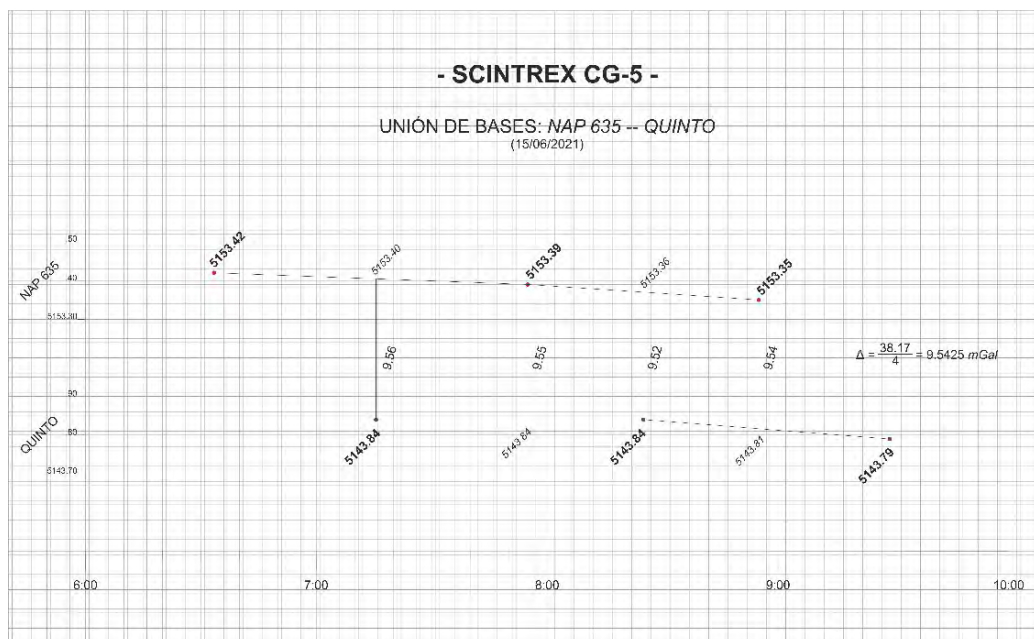


Figure 4. Linkage of NAP 635 and Quinto bases, showing the values taken to obtain the value of the new base at Quinto.

During the survey, it is necessary to control the static drift of the gravimeter. To control this drift we used a fixed point located in the IGME headquarters in Tres Cantos (Madrid, Spain). The control procedure measures the gravity at this point over several days. The figure 5 shows the graph with the test done in August 2021 which shows the good behaviour of the meter, displaying a good linearity with low drift during the periods of

measurement that correspond to the daily work program (around 8 hours). This behaviour indicates that the drift is within the expected values.

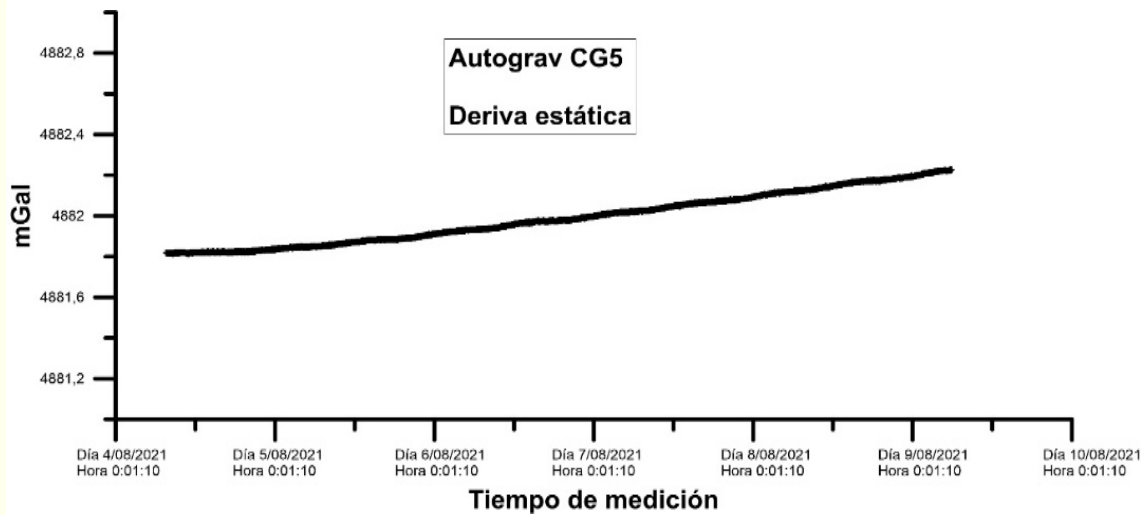


Figure 5. Static drift control of the Autograv Scintrex CG5 in Tres Cantos (Madrid, Spain) during the survey period. Axis X represents the time of the measurement, in days; Axis Y represents gravity in mGal.

### 2.2.1 Control of repetitions

Regarding the gravimetric measurements, and according to the norm (UNE 22-611-85), within this working scale of 1:10,000, the value of the root mean square error ( $E_{cm}$ ), for the observed gravity, must be less than  $\pm 0.06$  mGal. We carried out 75 repetitions that represent around 10.4% of the total measured stations. The statistics are represented in figure 6:

- 40 values (~53%) below 0.02 mGal difference.
- 22 values (~29%) between 0.02 mGal and 0.04 mGal difference.
- 9 values (~12%) between 0.04 mGal and 0.06 mGal difference.
- 4 values (~5%) between 0.06 mGal and 0.08 mGal difference.

The mean value of the differences is 0.022 mGal

The root mean square error of the repetitions is 0.024 mGal.

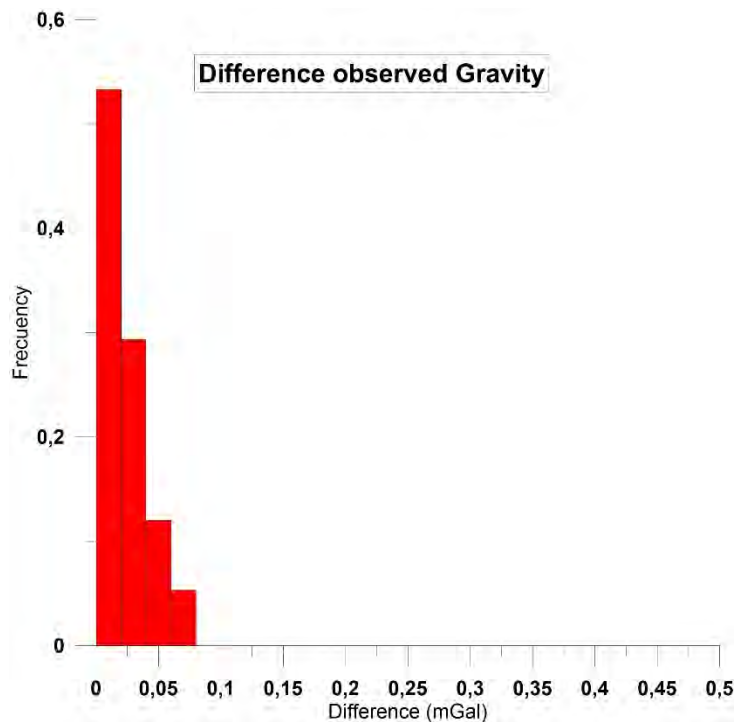


Figure 6. Difference for observed G values.

### 2.2.2 Calculation of observed gravity

The gravimeter used in this work measures relative values of gravity. The aim of a gravimetric survey is to measure the variation in the force of gravity between a specific point and the rest of the points in the surveyed area. This specific point is called the base: a point where the value of gravity is known.

The value of the gravity observed at a point is given by the following expression:

$$g_{obs} = ((I_p - I_b)k \pm CLS \pm D) + g_b$$

$g_{obs}$  = is the gravity observed at the measurement point p

$I_p$  = gravimeter reading at that point p

k = gravimeter calibration constant

CLS = Lunisolar Correction

D = gravimeter drift correction

$I_b$  = Gravimeter reading at the base

$g_b$  = Absolute gravity value at the base

D is the drift correction of the gravimeter. During the reading period, the gravimeter has variations due to mechanical and thermal effects, called the drift. To correct this drift we measured the difference between the reading at the base (opening time) and the reading at the base after one day of work (closing time). The drift is assumed to vary linearly with time, as shown on the graph in figure 5.

CLS is the lunisolar correction, which takes into account the influence of the moon and sun on the Earth's gravity. The Scintrex gravimeter provides the  $l_{pk}+CLS$  value, since it has a lunisolar correction calculation program implemented in the device. The formulas used for this calculation are based on the Longman equation (Longman, 1959) to predict the values of the tidal acceleration for a given time interval at any point on the Earth's surface.

The calculation of the observed gravity is carried out with an Excel Sheet, developed by the IGME.

### 2.3 Calculation of gravimetric anomalies

The objective of a gravimetric study is to determine the density distribution of the subsurface rocks by observing the disturbances that geological structures cause in the earth's gravitational field measured on the surface.

The gravimetric method is based on Newton's law of universal gravitation:

$$F = G \frac{m_1 m_2}{r^2}$$

where F is the gravitational pull between the masses  $m_1$  and  $m_2$ , r the distance between them and G the universal gravitational constant, whose value is  $(6.673 \pm 0.001) \cdot 10^{-11} \text{m}^3 \text{kg}^{-1} \text{s}^{-2}$

If  $m_2$  is the mass of the Earth, the acceleration acquired by the unit of mass located on the surface when subjected to the gravitational pull (F) is the acceleration due to gravity at the point where the mass is located (since  $F=m a$ ):

$$a=g=F/m_1 = Gm_2/r^2 \text{ (m/s}^2\text{)}$$

The value of observed gravity ( $g_{obs}$ ) depends on several factors: geographic latitude, station elevation, real distribution of densities under it and in its surroundings, and time (once corrected for drift and lunisolar variation).

This value must be compared with a theoretical value  $g_t$ , obtained from the normal gravity at the geoid as reference level ( $G_n$ ), but corrected to the elevation where  $g_{obs}$  has been measured. This correction involves the difference in height (z), the existing mass between those heights and the surrounding topography. The value B is called the Bouguer Anomaly and should depend exclusively on the ratio between theoretical and real densities.

$$B = g_{obs} - g_t$$

Processing the gravimetric data aims to obtain the value of the Bouguer Anomaly in each of the measurement points. By gridding all the Bouguer anomaly data we obtain the Bouguer anomaly map, which is the basis for the analysis and interpretation of the anomalies.

## 2.4 Calculation of the Bouguer anomaly

To obtain the Bouguer anomaly map we followed the indications and formulae from Hinze et al. (2005), as a routine procedure at IGME (e.g. Ayala et al., 2021). For the calculation we used the geodetic system GRS80 with orthometric heights and a density reduction of  $\rho=2.67\text{g/cm}^3$ . To process the data and obtain the final Bouguer Anomaly we used OASIS MONTAJ software from Seequent Company, complemented with some software developed by the IGME.

In order to choose the density reduction, we have calculated the Bouguer anomaly for different densities and correlated them with the elevation (Figure 7). In the figure, we observe a similar correlation between the different densities tested and the topography, so we cannot establish a clear value of density reduction. Thus, we have chosen  $2.67\text{ g/cm}^3$  because it is the standard value used in our institutional gravimetric data base, and it was used in previous gravimetric surveys close to this zone (Izquierdo-Llavall et al., 2019).

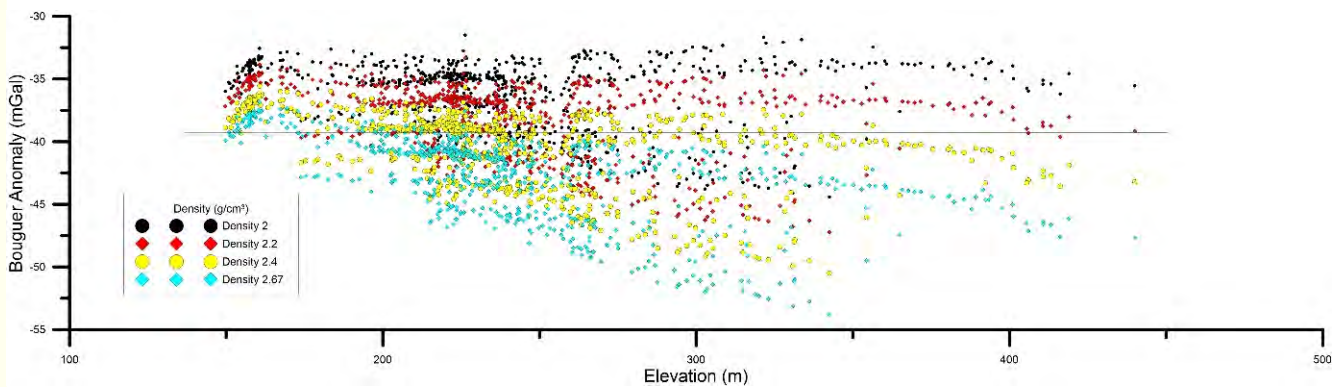


Figure 7. Correlation between the Bouguer anomaly and the elevation for different reduction density.

### 2.4.1 Normal gravity

Theoretical gravity is established from the normal gravity  $G_N$  existing on a reference surface or geoid (approximated by an ellipsoid of revolution), at sea level, and depends on the geographic latitude. In this work, we use the formula in the GRS80 geodetic reference system that uses the expression from Somigliana, 1929 developed in series (Moritz, 1984) for the normal gravity.

$$G_N = 978032.67715 * \left( \frac{1 + 0,001931851353 \sin^2(\lambda)}{\sqrt{1 - 0,0066943800229 \sin^2(\lambda)}} \right)$$

where  $\lambda$  is the latitude in the reference system.

#### 2.4.2 Altitude correction (free air correction)

Historically, the altitude correction has been called the free-air correction and it is defined as the difference between the gravity observed at a point on the surface of the Earth and the normal gravity on a reference surface: the ellipsoid or the geoid (Figure 8A).

In the case of the GRS80 system, the second order formula has been used, which improves the precision of the calculation and makes it dependent on the latitude and height of the station. Its expression is (Heiskanen and Moritz, 1967):

$$C_{AL} = - (0.3087691 - 0.0004398 \sin^2(\lambda)) * h + 7.2125 \cdot 10^{-8} * h^2$$

where  $h$  is the height in meters,  $\lambda$  is the latitude and  $C_{AL}$  is expressed in mGal.

#### 2.4.3 Bouguer correction

The Bouguer correction amends the effect of the gravitational attraction of the land mass between the vertical datum and the station. To calculate the effect of this mass, it is assumed to be an infinite layer of thickness  $h$  and density  $\rho$  (called the reduction density) (Figure 8B). The effect of that layer on the station is defined as:

$$\delta g_{BA} = 2\pi * G * h * \rho \text{ (mGal)}$$

where  $G$  is the universal gravitational constant,  $h$  is the height of the station in m, and  $\rho$  is the density of the layer in  $g/cm^3$ . Substituting the values of  $G$  and  $\pi$  we obtain:

$$\delta g_{BA} = 0.0419088 * h * \rho \text{ (mGal)}$$

#### 2.4.4 Terrain correction

Strictly speaking, the mass between the vertical datum and the station is not an infinite layer, but rather there is a topographical relief that presents excesses and defects of mass with respect to the layer (Figure 8C). To correct these mass excesses and defects, the terrain correction, CT, is calculated.

To apply the terrain correction, we followed the Hammer method of circular sectors (Hammer 1939), as the sum of the components: near, medium, distant and very distant. Near terrain correction (up to 170 m) was done in the field, by operator judgment and using Hammer tables. For the medium (up to 4,468.8 m), distant (up to 21,943 m) and very distant (up to 166.7 km) terrain correction, we used the CCT software (Plata, 1991, 2014), revised in 2019 together with the Institut Cartogràfic i Geològic de Catalunya. In the calculations, the height is in meters and the correction results in hundredths of milligal (cmGal).

For calculations, we used a 5x5 m grid from the IGN Digital Terrain Model (DTM), regrided to a 50 x 50 m grid for the medium and distant terrain correction (sectors E to M of Hammer). For corrections from sector M to 167 km (very distant) we used the 200 m grid of the IGN Digital Terrain Model regrided to a 400 x 400 m grid in the onshore Spanish territory; the onshore outside Spain was covered with data from MDS EUDEM of Copernicus; and for the offshore data we used bathymetric from the EMODnet database (<https://www.emodnet-bathymetry.eu/metadata-data>).

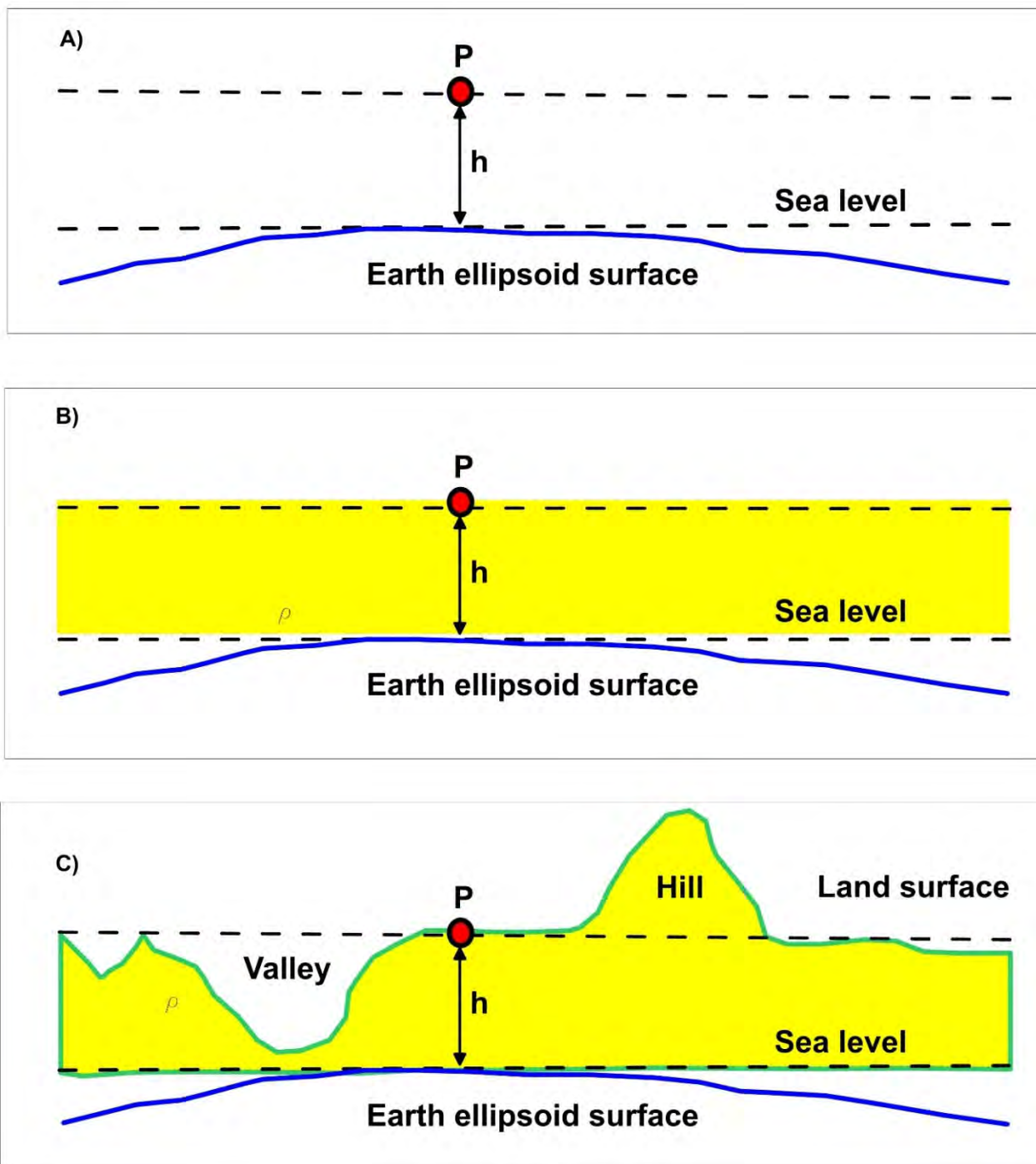


Figure 8. Scheme of the different corrections applied to obtain the Bouguer anomaly. A) Altitude correction; B) Bouguer correction; C) Terrain correction.

#### 2.4.5 Bouguer anomaly

The difference between the measured gravity and the theoretical gravity at a point on the surface is the Bouguer Anomaly, and it enables detecting the existence of variations in the acceleration of gravity produced by the density differences in the subsurface.

After applying the aforementioned corrections, the Bouguer anomaly is given by the following expression:

$$AB = g_{obs} - G_n + C_{AL} - \delta g_{BA} + CT$$

### 3. Analysis of gravimetric data

#### 3.1.1 Bouguer Anomaly map

After obtaining the values of the Bouguer anomaly for each point, we calculated a grid using the minimum curvature algorithm with a grid spacing of 500 x 500 m and we plotted the grid as equal intensity map using SURFER software (Figure 9).

The Bouguer gravity map shows the lateral density variations in the subsurface that are usually associated with lithological changes in the geological structures (e.g. basins, intrusions, etc.).

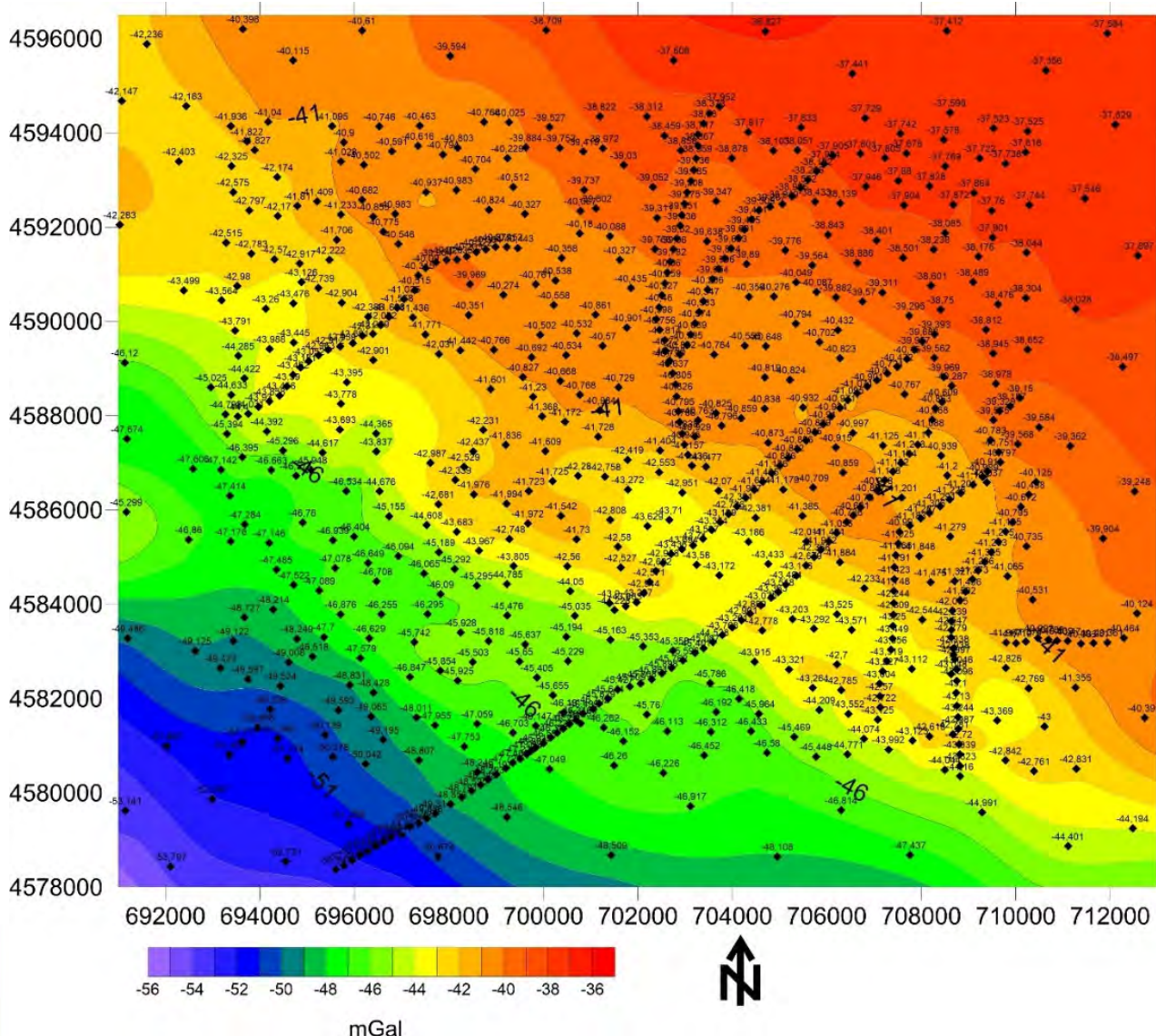


Figure 9. Bouguer Anomaly Map with reduction density 2.67 g/cm<sup>3</sup>. Isolines in mGal. The coordinates are UTM (ETRS89) H30N zone in meters.

### 3.1.2 Regional-Residual separation

The Bouguer anomaly map displays the superposition of anomalies produced by different sources at different depths. To interpret a gravimetric map in terms of the upper crustal structures, the first step, is to separate the regional anomalies (generally long wavelength that correspond to the contribution of the deeper sources) from the residual anomalies (shorter wavelength that reflects the contribution of shallower sources).

In this work, to calculate the regional anomaly we have used the polynomial adjust method using the REGRES software developed at IGME. With this software we obtain a polynomial adjust using the least squares algorithm directly over the data points. We can chose polynomials from degree 1 to 6. The polynomial represents the regional gravity anomaly and the residual gravity anomaly is obtained by subtracting from the Bouguer the regional anomaly.

We calculate the corresponding grids using Surfer software with the same parameters as we obtained the Bouguer anomaly grid.

Figure 10 shows the regional and residual anomalies obtained using polynomials of degrees 1, 2 and 3.

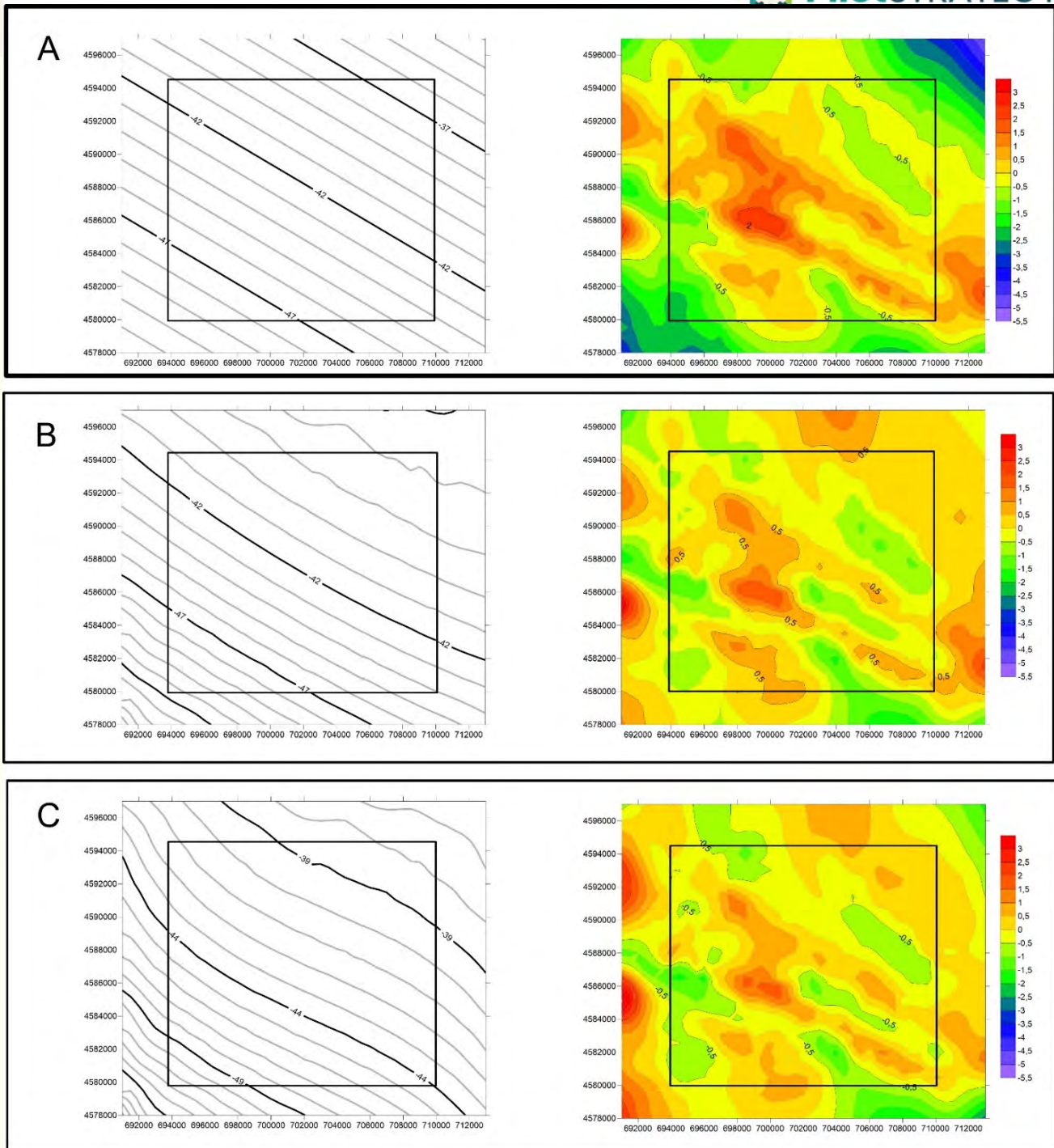


Figure 10. On the left regional anomaly map from fitting the degrees 1 (A), 2 (B) and 3 (C) polynomial surfaces. At the right hand side the residual Bouguer maps obtained by subtracting the regional from the Bouguer anomaly maps. The inner rectangle indicates the area of interest with more density in measured data. Isolines and colour scale in mGal. UTM coordinates (ETRS89) H30N zone in meters.

## 4. Interpretation

The Bouguer anomaly map depicts a clear gradient SW-NE as the regional trend in the area (see Figure 9). The three residual anomaly maps (Figure 10) show two elongated maxima with a NW-SE trend and some lineaments (1 and 2 in figure 11) that are connected in the centre by a NE-oriented high (A in Figure 11). They extend to the southeast with a diminished amplitude signal. Related to those, another anomaly (lineament 6 in Figure 11), also NW-SE trend, can be associated to lineaments 1 and 2. Interrupting the NW-SE trending anomalies there are some less conspicuous anomalies with a NE-SW trend (lineaments 3, 4 and 5 in Figure 11).

We have calculated the power spectrum of each of the three residual anomalies using Oasis Montaj software (figure 12) which provides the source depth of the anomalies. The depth obtained using the residual of degree 1 (Fig. 12A) is ca. 2 km whereas for the other residuals (degree 2 and 3) the depth is lesser (about 1.5 km). The seismic profiles indicate that the structures of interest lie at a depth of about 2 km, supporting the election of the first degree polynomial as the regional trend to subtract. Furthermore, if we compare the isobath map obtained from the seismic profiles in 2015 (Figure 1C, the Variscan basement is 150 m below the Buntsandstein) and three residual anomalies (Figure 10), it shows a greater similarity with the 1 degree residual. Thus, in the SW and NE margins of the area, a progressive increase in the depth of the basement is observed, which correspond to gravimetric minimums in the first degree polynomial and, on the contrary, the residuals of 2 or 3 degrees are not observed.

Moreover, in the general geological context of this study, we can conclude that while the NW-SE trend is related to the Iberian Range, outcropping southwest of this area, the NE-SW trend are less evident and may reflect the Catalanian Coastal Range trend.

The correlation between this gravity survey and the geology of the area, together with the subsurface information, will be carried out later in the frame of the work package aiming to obtain the final geological model.

This gravimetric study constitutes the basis of the forthcoming geophysical-geological modelling, which will endorse the global characterization of the Lopín structure and will help to choose the final CO<sub>2</sub> storage site.

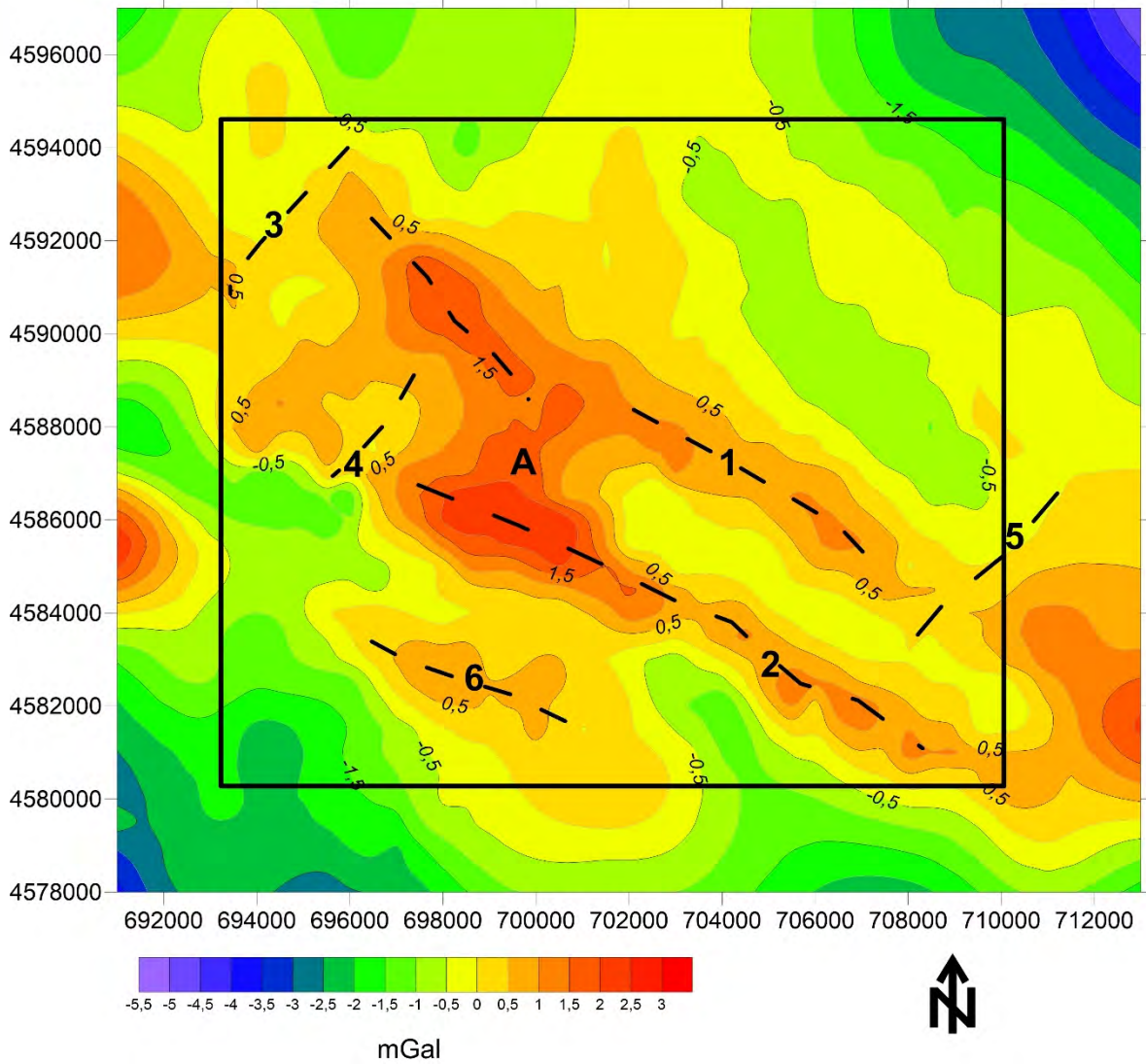
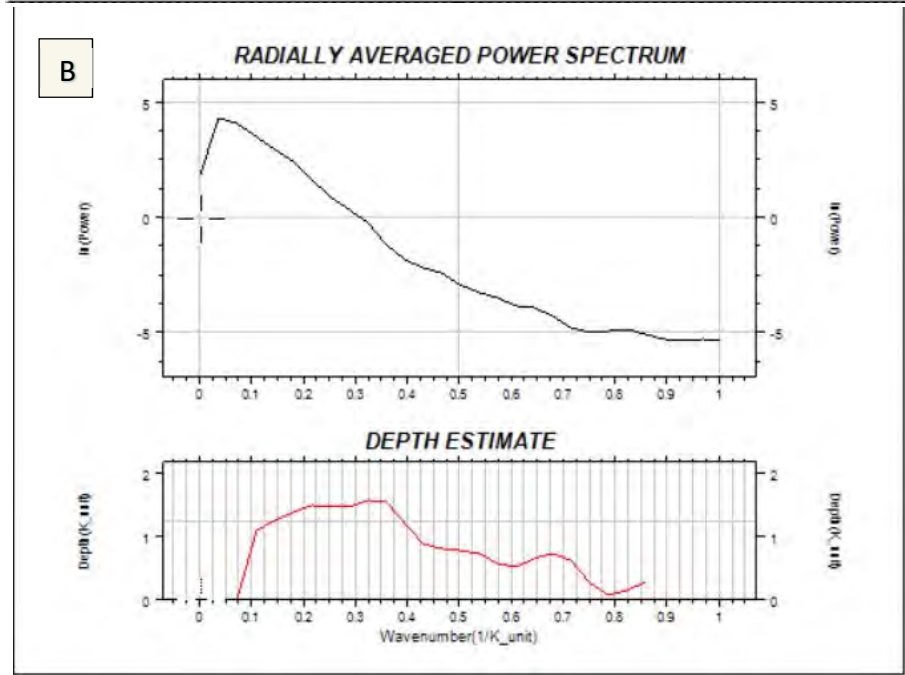
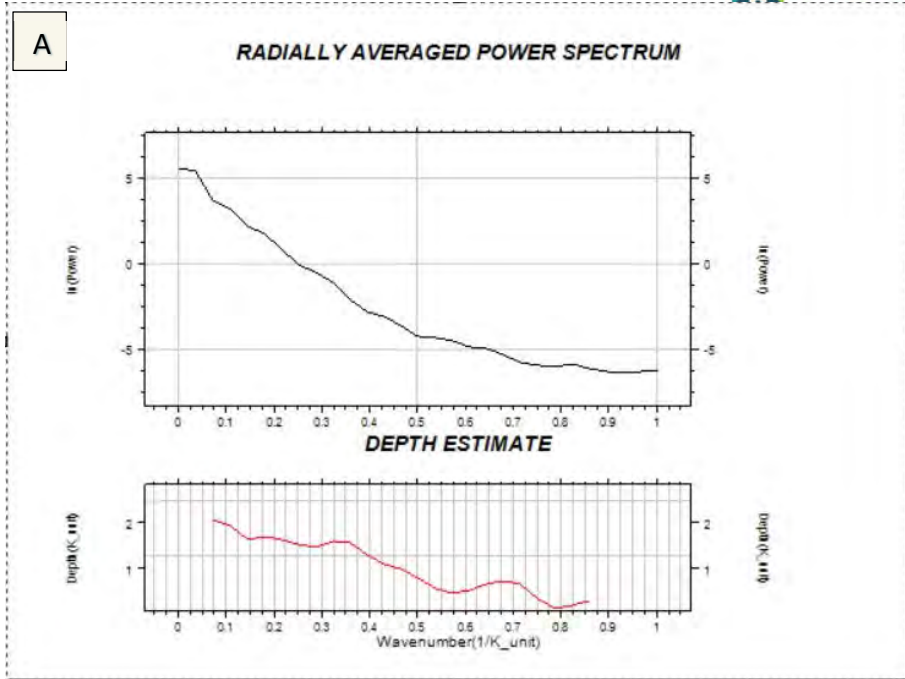


Figure 11. Residual map of Bouguer anomaly, derived from the subtraction of the regional anomaly of degree 1 from the Bouguer anomaly. The inner rectangle indicates the area of interest with more density in measured data. NW-SE and NE-SW interpreted trends are overlaid. Isolines in mGal. UTM coordinates (ETRS89) H30N zone in meters.



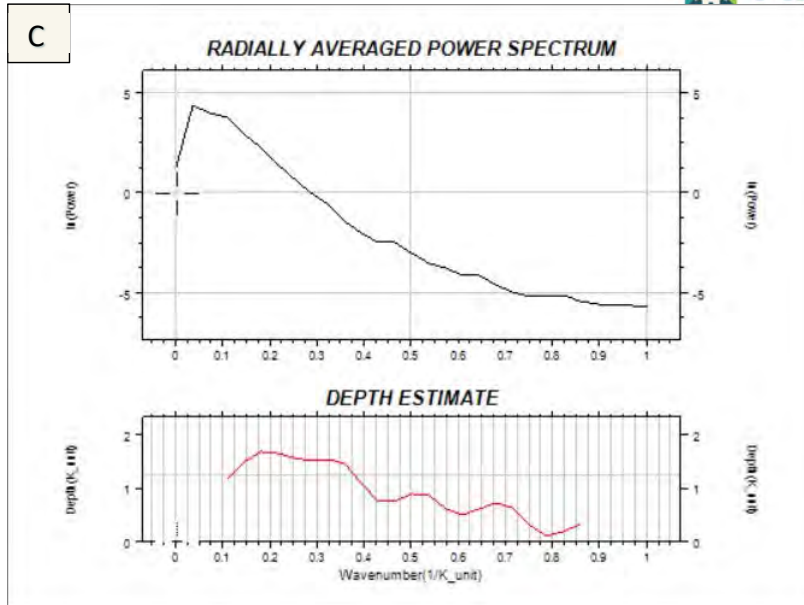


Figure 12. Radially averaged power spectrum and depth estimation for residual of degree 1 (A), degree 2 (B) and degree 3 (C).

## 5. References

- Ayala, C., Rey-Moral, C., Rubio, F., Soto, R., Clariana, P., Martín-León, J., Bellmunt, F., Gabàs, A., Macau, A., Casas, A.M., Martí, J., Pueyo, E.L. and Benjumea, B., 2021. Gravity data on the Central Pyrenees: a step forward to help a better understanding of the Pyrenean structures. *Journal of Maps*, 17:2, 891-900. DOI: 10.1080/17445647.2021.2001386.
- Hammer S., 1939. Terrain corrections for gravimeter stations. *Geophysics*, 4: 184-194. <https://doi.org/10.1190/1.1440495>.
- Heiskanen W.A., Moritz H., 1967. *Physical geodesy*. Freeman, San Francisco.
- Hinze, W. J. , C. Aiken, J. Brozena, B. Coakley, D. Dater, G. Flanagan, R. Forsberg, T. Hildenbrand, G. R. Keller, J. Kellogg, D. Plouff, D. Ravat, D. Roman, J. Urrutia-Fucugauchi, M. Véronneau, M. Webring, D. Winester, 2005. New standards for reducing gravity data: the North American gravity database, *Geophysics*, 70, no. 4, p. J25-J32.
- Izquierdo-Llavall, E., Ayala, C., Pueyo, E.L., Casas, A.M., Oliva-Urcía, B., Rubio, F.M., Rodríguez-Pintó, A., Rey-Moral, C., Mediato, J.F. y García-Crespo, J., 2019. Basement-cover relationships and their along-strike changes in the Linking Zone (Iberian Range, Spain): a combined structural and gravimetric study. *Tectonics*, 38. DOI: 10.1029/2018TC005422.
- Longman I.M., 1959. Formulas for computing the tidal accelerations due to the Moon and the Sun. *Journal of Geophysical Research*, 64(12): 2351–2355.
- Mediato José F., García-Crespo Jesús, Ayala Concepción, Izquierdo Esther, García-Lobón José L., Rubio Félix, Rey-Moral Carmen, Pueyo Emilio, 2015. Geological modelling of the Lopín CO<sub>2</sub> storage site, Spain. 8<sup>th</sup> EUREGEO, Barcelona (Spain) Geological 3D Modelling – Posters.
- Moritz H, 1984. The geodetic reference system 1980. *Bull Geod* 58(3): 388-398.
- Plata, J.L., 2014. Manual program CCT BLOQUES. IGME, informe inédito Área Geofísica.
- Somigliana C., 1929. Teoría generale del campo gravitazionale dell' ellipsoide di rotazione. *Mem. Soc. Astron. Ital.*, IV.

## 6. Annex






# ARAGEA

## Estación permanente de Quinto (QNTO)

**UBICACIÓN**

Código estación: QNTO

Nombre RINEX3: QNTO3

Nombre: Quinto

DOMES: 19363M001

Redes Pertenece: ARAGEA

Instituciones Pertenece: IGEAR

Localización: Avda. Constitución 20, 50770 Quinto (Zaragoza) ARAGÓN

Fecha Instalación: 15/12/2009

Tipo instalación: Mástil de 1,5m. Anclado a tejado de dos aguas, reforzado con vientos. Nivelada y orientada al norte.



**COORDENADAS ETRS89**

**INSTRUMENTACIÓN**

| Cartesianas<br>(x, y, z) | Geográficas<br>(φ, λ, h) | UTM<br>(x,y,huso) |
|--------------------------|--------------------------|-------------------|
| 4789431,3968             | 41° 25' 32,17196" N      | 709159,511        |
| -41541,0552              | 0° 29' 48,98958" W       | 4589028,738       |
| 4198123,6593             | 216,666 m.               | 30                |

Receptor: LEICA GR50

Antena: GNSS Choke Ring CR-G3

Altura Antena: 0 metros.

Observaciones: GPS, GLONASS, GALILEO y BEIDOU

Frecuencias: L1, L2 y L2C

**INFORMACIÓN ADICIONAL**

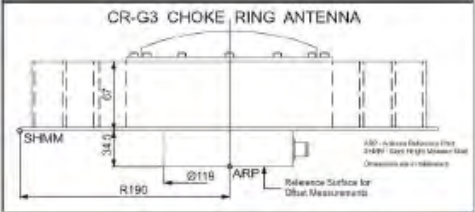
Rinex Horarios cada 1 segundo, y Diarios cada 30 segundos.

Casos NTRIP: <http://ntrip.aragon.es:2101>

RINEX y LOG: <http://gnss.aragon.es>

e-mail / Web: [aragea@aragon.es](mailto:aragea@aragon.es) / <http://gnss.aragon.es>

Última actualización: 16/12/2020



**FOTOS**






Figure 1. Permanent GNSS station of Quinto from the GNSS network of the Gobierno de Aragón (ARAGEA)

“(A)”

ARAGEA

## Estación permanente de Zaragoza (ZGZA)

### UBICACIÓN

Código estación: ZGZA  
 Nombre RINEX3: ZGZA3  
 Nombre: Zaragoza  
 DONES: 13462M002  
 Redes Pertenece: ARAGEA  
 Instituciones Pertenece: IGEAR  
 Localización: Pza. San Pedro Nolasco 7, 50071 Zaragoza (Zaragoza) ARAGÓN



Fecha Instalación: 26/09/2013

Tipo Instalación: mástil de acero galvanizado de 1,5m. Anclado a pared y terminado en tornillo y tuerca de 5/8". Nivelada y orientada al norte.

### COORDENADAS ETRS89

| Cartesianas (x, y, z) | Geográficas (φ, λ, h) | UTM (x, y, huso) |
|-----------------------|-----------------------|------------------|
| 4772401,6196          | 41° 39' 8,27722" N    | 676844,854       |
| -72990,2582           | 0° 52' 34,41762" W    | 4613351,391      |
| 4217009,9737          | 276,778 m.            | 30               |

### INSTRUMENTACIÓN

Receptor: LEICA GR30  
 Antena: Leica AR10 (LEIAR10 NONE)  
 Altura Antena: 0 metros.  
 Observaciones: GPS, GLONASS, GALILEO y BEIDOU  
 Frecuencias: L1, L2 y L2C

### INFORMACIÓN ADICIONAL

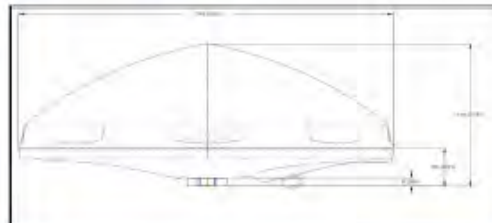
Rinex Horarios cada 1 segundo, y Diarios cada 30 segundos.

Ceser NTRIP: <http://ntrip.aragon.es:2101>

RINEX y LOG: <http://gnss.aragon.es>

e-mail / Web: [aragea@aragon.es](mailto:aragea@aragon.es) / <http://gnss.aragon.es>

Última actualización: 16/12/2020



### FOTOS



Figure 2. Permanent GNSS station of Zaragoza from the GNSS network of the Gobierno de Aragón (ARAGEA)

### Reseña de Señal de Nivelación

13-nov-2021

**Situación Geográfica:**  
**Número:** 810035  
**Nombre:** NGAB 635  
**Línea o Ramal:** 810. Zaragoza - Alcorisa  
  
**Municipio:** Zaragoza  
**Provincia:** Zaragoza  
**Hoja MTN50:** 384  
**Señal:** Principal      **En posición:** Horizontal  
**Señalizada:** 15 de abril de 2008  
**Nivelada:**

**Enlaces:**  
**Anterior:** 810154 - SSK 17,58  
**Posterior:** 810036 - SSK 1,3  
**Agrupada con:**

**Datos Geodésicos:**  
**Altitud ortométrica:** 210,4265 m.  
**Geopotencial:** 206,2676 u.g.p.  
**Gravedad en superficie:** 980227,09 mgals.      *Observada*  
**Cálculo:**

**Coordenadas Geográficas ETRS89:**  
**Longitud:** - 0° 41' 48,6546"  
**Latitud:** 41° 32' 16,8927"  
**Altitud elipsoidal:** 260,377 m.  
**Precisión:** ± 0,05 m.

**Reseña:**  
 Clavo metálico cuya cabeza tiene grabada la inscripción NGAB 635 incrustado aproximadamente en el Km. 0,800 de la margen Oeste de la Carretera A-222, sobre el paramento Este de un bunker de hormigón, unos 8 metros al Oeste de la carretera antigua, según croquis. Dista unos 1160 m. de la señal número 810 154.



**Observaciones:**

Informe del estado de la Señal en: <http://tp.geodesia.ign.es/Utilidades/InfoRN.pdf>

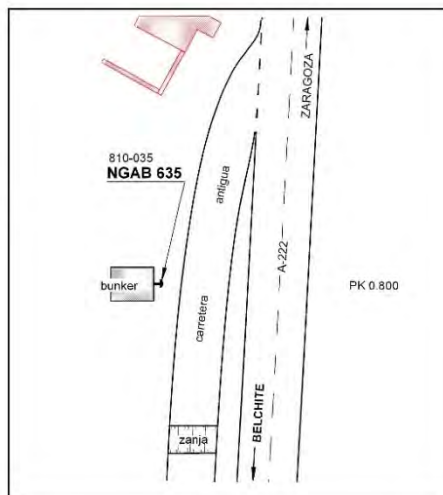


Figure 3. Review of the gravimetric base station NGAB 635 from the IGN REDNAP network.

## Reseña Base Gravimétrica

### Situación Geográfica:

Nombre: Quinto  
Municipio: Quinto  
Provincia: Zaragoza  
Hoja MTNSO: 413  
Señalizada: 15 junio 2021

### Datos Geodésicos:

Gravedad observada: 980217.5475 mGal  
Cálculo: 15 junio 2021

### Coordenadas UTM:

Sistema de Ref: ETRS89  
X: 708645.641  
Y: 4588632.870  
Huso: 30  
Z elipsoidal: 246.633  
Z ortométrica: 196.781

### Reseña:

Enlace de bases empleando la base número 810035 (nombre NGAB 635) situada en km 0.800 del margen oeste de la carretera A-222 sobre el paramento este de un bunker de hormigón junto a la carretera antigua.

La nueva base se encuentra en el cementerio de Quinto (recinto del limbo) a la izquierda de una placa conmemorativa.



Figure 4. Review of the gravimetric base station of Quinto established for this survey and linked to the NGAB 635 base station from the IGN REDNAP network.